

SUPPORTING INFORMATION

Chiral cyanido-bridged Mn–Nb magnets with halogen-bonds

Ohno Takuro,[†] Koji Nakabayashi,[†] Kenta Imoto,[†] Masaya Komine,[†], Szymon Chorazy,[‡]

and Shin-ichi Ohkoshi^{†,}*

[†]Department of Chemistry, School of Science, The University of Tokyo, 7-3-1 Hongo, Bunkyo-ku,

Tokyo 113-0033, Japan.

[‡]Faculty of Chemistry, Jagiellonian University, Gronostajowa 2, 30-387 Kraków, Poland.

1.	Experimental details	S2–3
2.	Crystal data and structure refinement (Table S1)	S4–5
3.	Detailed structural parameters (Table S2)	S6–9
4.	Results of Continuous Shape Measures (CShM) Analysis (Table S3)	S10
5.	Helix of the Mn-Nb-4-Brpy network at 90 K (Figure S1)	S11
6.	Crystal structure of 2 at 90 K (Figure S2)	S12
7.	Powder X-ray diffraction patterns of 1 and 2 (Figure S3)	S13
8.	UV-Vis diffuse reflectance spectra of 1 and 2 (Figure S4)	S14
9.	IR spectra of 1 and 2 (Figure S5)	S15
10.	Thermogravimetric measurements for 1 (a) and 2 (Figure S6)	S16
11.	Temperature dependence of χ_{MT} of 1 (Figure S7)	S17
12.	Temperature dependence of χ_{MT} of 2 (Figure S8)	S17
13.	Tensor elements of the SH susceptibility for 1 and Mn-Nb-4-Brpy network.	S18
14.	SH light intensity vs fundamental light intensity plots of 1 and Mn-Nb-4-Brpy network (Figure S9)	S19
15.	References to Supporting Information	S20

EXPERIMENTAL DETAILS

Syntheses.

[Mn^{II}(4-iodopyridine)₄]₂[Nb^{IV}(CN)₈] (1)

(Powder sample) MnCl₂·4H₂O (0.4 mmol), L-ascorbic acid sodium salt (0.8 mmol), and 4-iodopyridine (1.6 mmol) were dissolved in a mixed solution of 24 mL of ethanol and 20 mL of water and a 4 mL aqueous solution of K₄[Nb^{IV}(CN)₈]·2H₂O (0.2 mmol) were added. After 1 h stirring, yellow polycrystalline sample of **1** were filtrated and washed by water. Yield, 350.1 mg, 80 % (based on Nb atom). Elemental analyses showed that the formula is C₄₈H₃₂I₈Mn₂N₁₆Nb₁ (*M_w* = 2051 g mol⁻¹. Calcd: C, 28.11 %; H, 1.57 %; Mn, 5.36 %; N, 10.93 %; Nb, 4.53 %. Found: C, 28.26 %; H, 1.97 %; Mn, 5.52 %; N, 10.90 %; Nb, 4.69 %.).

(Single crystal) Single crystals of **1** were obtained from a water–ethanol solution (1:1, v/v) of MnCl₂·4H₂O, L-ascorbic acid sodium salt, and 4-iodopyridine slowly reacting with an aqueous solution of K₄[Nb^{IV}(CN)₈]·2H₂O.

[Mn^{II}(4-chloropyridine)₄]₂[Nb^{IV}(CN)₈]·0.5H₂O (2)

(Powder sample) MnCl₂·4H₂O (0.44 mmol), L-ascorbic acid sodium salt (1 mmol), potassium hydroxide (4 mmol), and 4-chloropyridine hydrochloride (4 mmol) were dissolved in 32 mL of water and a 8 mL aqueous solution of K₄[Nb^{IV}(CN)₈]·2H₂O (0.2 mmol) were added. After 1 h stirring, yellow polycrystalline sample of **2** were filtrated and washed by small amount of water, then dried under Ar-gas flowing for 30 minutes. Yield, 190 mg, 72 % (based on Nb atom). Elemental analyses showed that the formula is C₄₈H₃₃Cl₈Mn₂N₁₆Nb₁O_{0.5} (*M_w* = 1328.7 g mol⁻¹. Calcd: C, 43.39 %; H, 2.50 %; Mn, 8.27 %; N, 16.87 %; Nb, 7.00 %. Found: C, 43.41 %; H, 2.45 %; Mn, 7.97 %; N, 16.88 %; Nb, 7.21 %.).

(Single crystal) Single crystals of **2** were obtained from an aqueous solution of MnCl₂·4H₂O, L-ascorbic acid sodium salt, potassium hydroxide, and 4-chloropyridine hydrochloride slowly reacting with a water–ethanol solution (1:1, v/v) of K₄[Nb^{IV}(CN)₈]·2H₂O.

Crystal Structure Determination

For single crystal X-ray diffraction measurements of **1** and Mn-Nb-4-Brpy network, the enantiomers were selected from the mixture of the crystals with (+) and (-) structures. Single Crystal X-ray crystal structural analyses were conducted by Rigaku RAXIS RAPID imaging plate area detector, equipped with graphite monochromated MoK α radiation with the crystals protected by Paratone N oil and mounted on pen tips. Measurements were done at room temperature and 90 K. The structures were solved by using SIR-2014, SIR-92^{S1} or SHELXS-2013 software, and refined by using SHELXL-2014/7 software.^{S2} The analyses were conducted on Rigaku Crystal Structure and WinGX (ver. 1.80.05) software.^{S3} All non-hydrogen atoms except solvent water molecules suggested by elemental analyses were found independently and refined with anisotropic temperature factor. In the refinement of **1**, since preliminary analysis where twinning was not assumed showed irrational structural model, a twinning with a 2-fold rotation along [0 1 0] as twin element were assumed. Because compound **1** showed noncentrosymmetric structure, the analyses were conducted with 4 twin domains. Hydrogen atoms belonging to 4-iodopyridine and 4-chloropyridine ligands were introduced

by the idealized positons with riding model. The solvent molecules could not be determined for the possible structural disorders. Structural figures were created by The PyMOL Molecular Graphics System, Version 1.2 Schrödinger, LLC. The continuous shape measures of Nb and Mn atomic sites were conducted by SHAPE software ver. 2.1.^{S4}

Physical Techniques.

Elemental analyses were conducted by using Agilent 7700 ICP-MS for metals (Mn, Nb) by the standard microanalytical method for C, H, and N atoms. The PXRD patterns were obtained by using Rigaku Ultima IV diffractometer. Absorption spectra were measured by JASCO V-670 spectrometer employing diffuse reflectance method on samples mixed in BaSO₄ for UV-Vis-NIR, and JASCO FT/IR 4100 spectrometer employing KBr pellet method for IR. Thermogravimetric measurement was conducted by RIGAKU Thermo Plus TG8120 in the 27 – 450°C range at a heating rate of 2 °C min⁻¹. Magnetic properties measurements were conducted with Quantum Design MPMS SQUID magnetometer.

SHG measurement.

A frequency doubled 775 nm Ti:sapphire laser (Clark-MXR CPA-2001) was used as the fundamental light. The fundamental light, which passed through neutral density filters and longpass filters, was focused and irradiated to samples. The reflected light was passed through blue filters and THG cut filters, and focused into a photomultiplier tube (Hamamatsu R464) equipped with a band pass filter.

Table S1. Crystal Data and Structural Refinement

compound	1(+)		1(-)		2	
formula	C ₄₈ H ₃₂ I ₈ Mn ₂ N ₁₆ Nb ₁	C ₄₈ H ₃₂ I ₈ Mn ₂ N ₁₆ Nb ₁	C ₄₈ H ₃₂ I ₈ Mn ₂ N ₁₆ Nb ₁	C ₄₈ H ₃₂ I ₈ Mn ₂ N ₁₆ Nb ₁	C ₄₈ H ₃₂ Cl ₈ Mn 2N ₁₆ Nb ₁ O _{0.5}	C ₄₈ H ₃₂ Cl ₈ Mn 2N ₁₆ Nb ₁ O _{0.5}
formula weight [g·mol ⁻¹]	2050.89	2050.89	2050.89	2050.89	1328.73	1328.73
crystal size [mm × mm × mm]	0.23×0.21×0. 21	0.23×0.21×0. 21	0.23×0.20×0. 20	0.17×0.15×0. 10	0.18×0.11×0. 11	0.18×0.11×0. 11
<i>T</i> [K]	300	90	295	90	296	90
crystal system	tetragonal	tetragonal	tetragonal	tetragonal	orthorhombic	orthorhombic
space group	<i>I</i> 4 ₁	<i>I</i> 4 ₁	<i>I</i> 4 ₁	<i>I</i> 4 ₁	<i>Fddd</i>	<i>Fddd</i>
<i>a</i> [Å]	20.8730(7)	20.7954(7)	20.8811(9)	20.792(2)	13.9379(3)	13.7697(5)
<i>b</i> [Å]	20.8730(7)	20.7954(7)	20.8811(9)	20.792(2)	26.6853(5)	26.2046(9)
<i>c</i> [Å]	14.2157(4)	14.1103(5)	14.2190(4)	14.1122(7)	31.5931(6)	31.9937(12)
<i>V</i> [Å ³]	6193.5(5)	6102.0(5)	6199.8(6)	6100.8(12)	11750.6(4)	11544.3(7)
<i>Z</i>	4	4	4	4	8	8
calculated density [g·cm ⁻³]	2.199	2.232	2.197	2.233	1.491	1.518
absorption coefficient [mm ⁻¹]	4.617	4.687	4.613	4.688	1.027	1.045
<i>F</i> (000)	3788.0	3788.0	3788.0	3788.0	5272.0	5272
θ range [deg.]	3.086– 27.460	3.098– 27.472	3.085– 27.471	3.098– 27.483	3.053– 27.479	3.110– 27.480
<i>hkl</i> indices	–24< <i>h</i> <27 –27< <i>k</i> <27 –18< <i>l</i> <18	–23< <i>h</i> <26 –26< <i>k</i> <24 –18< <i>l</i> <18	–27< <i>h</i> <25 –26< <i>k</i> <27 –18< <i>l</i> <18	–26< <i>h</i> <26 –26< <i>k</i> <26 –18< <i>l</i> <18	–18< <i>h</i> <17 –34< <i>k</i> <34 –40< <i>l</i> <40	–17< <i>h</i> <17 –34< <i>k</i> <33 –41< <i>l</i> <41
observed reflections	43746	48185	43344	46794	37235	44534
symmetry– independent reflections	7084	6988	6964	6889	3378	3310
<i>R</i> _{int}	0.038	0.032	0.0421	0.064	0.044	0.034
completeness	0.995	0.997	0.997	0.997	0.999	0.999
data/restraints/para meters	7084/33/342	6988/7/342	6964/5/342	6889/29/342	3378/0/172	44534/0/172
GOF on <i>F</i> ²	1.142	1.062	1.087	1.090	1.368	1.481
<i>R</i> [<i>F</i> ² > 2σ(<i>F</i> ²)]	0.0458	0.0217	0.0455	0.0270	0.0589	0.0453
<i>wR</i> (<i>F</i> ²)	0.1144	0.0526	1.088	0.0652	0.1080	0.0702
largest diff peak/hole [e·Å ⁻³]	2.131/ –1.657	1.571/ –0.834	2.008/ –1.416	0.964/ –0.891	0.487/ –0.692	0.476/ –0.443

Table S1. Crystal Data and Structural Refinement (continued)

compound	Mn-Nb-4-Brpy network (+)	Mn-Nb-4-Brpy network (-)
formula	C ₄₈ H ₃₃ Br ₈ Mn ₂ N ₁₆ Nb ₁ O _{0.5}	C ₄₈ H ₃₃ Br ₈ Mn ₂ N ₁₆ Nb ₁ O _{0.5}
formula weight [g·mol ⁻¹]	1674.89	1674.89
crystal size [mm × mm × mm]	0.33×0.29×0.18	0.26×0.10×0.09
<i>T</i> [K]	90	90
crystal system	tetragonal	tetragonal
space group	<i>I</i> 4 ₁ 22	<i>I</i> 4 ₁ 22
<i>a</i> [Å]	20.5345(12)	20.5122(11)
<i>b</i> [Å]	20.5345(12)	20.5122(11)
<i>c</i> [Å]	13.8992(4)	13.9053(4)
<i>V</i> [Å ³]	5860.8(7)	5850.7(6)
<i>Z</i>	4	4
calculated density [g·cm ⁻³]	1.898	1.901
absorption coefficient [mm ⁻¹]	6.119	6.130
<i>F</i> (000)	3212.0	3212.0
θ range [deg.]	3.137–27.479	3.141–27.477
<i>hkl</i> indices	-26 < <i>h</i> < 26 -26 < <i>k</i> < 26 -18 < <i>l</i> < 18	-26 < <i>h</i> < 26 -26 < <i>k</i> < 26 -18 < <i>l</i> < 18
observed reflections	45398	47004
symmetry-independent reflections	3347	3353
<i>R</i> _{int}	0.0699	0.0885
completeness	0.997	0.996
Flack <i>x</i> parameter	0.109(3)	0.077(4)
data/restraints/parameters	3347/0/174	3357/7/174
GOF on <i>F</i> ²	1.571	0.954
<i>R</i> [<i>F</i> ² > 2σ(<i>F</i> ²)]	0.0202	0.0420
<i>wR</i> (<i>F</i> ²)	0.423	0.0485
largest diff peak/hole [e·Å ⁻³]	0.310/-0.510	1.045/-0.656

Table S2. Detailed Structural Parameters

compound	1(+)	1(-)
Temperature	90	90
Halogen Bonding		
N3···I17 [Å]	3.107(8)	3.106(9)
∠N3···I17 – C14 [°]	166.0(3)	166.5(3)
N4···I27	3.044(7)	3.061(8)
∠N4···I27 – C24	176.5(3)	176.5(3)
[Nb ^{IV} (CN) ₈] moiety		
Nb1 – C1	2.227(7)	2.246(9)
Nb1 – C2	2.238(8)	2.223(8)
Nb1 – C3	2.287(9)	2.287(9)
Nb1 – C4	2.269(8)	2.287(9)
C – N (bonding)	1.154(10), 1.152(11)	1.146(11), 1.146(11)
C – N (terminal)	1.111(12), 1.157(11)	1.122(12), 1.118(12)
∠Nb1 – C1 – N1	178.4(7)	179.4(8)
∠Nb1 – C2 – N2	179.8(8)	179.0(8)
∠Nb1 – C3 – N3	175.8(7)	179.0(8)
∠Nb1 – C4 – N4	179.8(8)	174.8(8)
[Mn ^{II} (4-Ipy) ₄ (NC) ₂] moiety		
Mn1 – N1 (CN)	2.153(7)	2.156(7)
Mn1 – N2 (CN)	2.160(7)	2.167(8)
Mn1 – N11 (Ipy)	2.298(7)	2.301(8)
Mn1 – N21 (Ipy)	2.307(7)	2.311(8)
Mn1 – N31 (Ipy)	2.308(7)	2.310(8)
Mn1 – N41 (Ipy)	2.313(6)	2.301(7)
∠Mn1 – N1 – C1	174.1(7)	164.6(7)
∠Mn1 – N2 – C2	164.5(6)	173.4(7)
∠N1 – Mn1 – N2	177.4(3)	177.1(3)
∠N11(Ipy) – Mn – N21(Ipy)	172.6(2)	173.1(3)
∠N11(Ipy) – Mn – N31(Ipy)	94.3(3)	92.6(3)
∠N11(Ipy) – Mn – N41(Ipy)	85.0(3)	88.2(3)
∠N21(Ipy) – Mn – N31(Ipy)	93.1(3)	94.3(3)
∠N21(Ipy) – Mn – N41(Ipy)	87.6(3)	85.0(3)
∠N31(Ipy) – Mn – N41(Ipy)	178.6(3)	178.2(3)
∠N(Ipy) – Mn – N(CN)	87.3(3) – 91.6(3)	86.9(3) – 91.5(3)

Table S2. Detailed Structural Parameters (continued)

compound	1(+)	1(-)
Temperature	300	295
Halogen Bonding		
N3···I17	3.086(14)	3.090(15)
∠N3···I17 – C14	177.3(6)	176.9(6)
N4···I27	3.199(16)	3.189(15)
∠N4···I27 – C24	166.7(7)	166.4(7)
[Nb ^{IV} (CN) ₈] moiety		
Nb1 – C1	2.208(17)	2.230(19)
Nb1 – C2	2.289(12)	2.266(12)
Nb1 – C3	2.258(13)	2.295(16)
Nb1 – C4	2.25(2)	2.245(16)
C – N (bonding)	1.18(2), 1.069(17)	1.17(2), 1.094(19)
C – N (terminal)	1.18(2), 1.13(3)	1.14(2), 1.14(2)
∠Nb1 – C1 – N1	172.2(15)	173.1(15)
∠Nb1 – C2 – N2	176.2(11)	177.0(11)
∠Nb1 – C3 – N3	177.1(13)	178.0(15)
∠Nb1 – C4 – N4	173(2)	174.7(17)
[Mn ^{II} (4-Ipy) ₄ (NC) ₂] moiety		
Mn1 – N1 (CN)	2.168(15)	2.154(12)
Mn1 – N2 (CN)	2.192(13)	2.195(15)
Mn1 – N11 (Ipy)	2.328(14)	2.321(15)
Mn1 – N21 (Ipy)	2.297(15)	2.316(12)
Mn1 – N31 (Ipy)	2.313(14)	2.307(14)
Mn1 – N41 (Ipy)	2.324(10)	2.323(10)
∠Mn1 – N1 – C1	169.8(13)	171.5(12)
∠Mn1 – N2 – C2	170.6(12)	170.8(12)
∠N1 – Mn1 – N2	177.2(4)	177.6(4)
∠N11(Ipy) – Mn – N21(Ipy)	173.9(4)	173.3(5)
∠N11(Ipy) – Mn – N31(Ipy)	92.6(6)	91.4(6)
∠N11(Ipy) – Mn – N41(Ipy)	87.1(6)	86.5(7)
∠N21(Ipy) – Mn – N31(Ipy)	93.3(7)	94.6(6)
∠N21(Ipy) – Mn – N41(Ipy)	87.0(7)	87.5(7)
∠N31(Ipy) – Mn – N41(Ipy)	179.7(9)	177.2(7)
∠N(Ipy) – Mn – N(CN)	87.8(6) – 92.0(6)	86.4(6) – 91.9(5)

Table S2. Detailed Structural Parameters (continued)

compound	2	2
Temperature	296	90
Halogen Bonding		
N2...Cl3	3.281(4)	3.183(2)
\angle N2...Cl3 – C10	168.98(18)	166.79(10)
[Nb ^{IV} (CN) ₈] moiety		
Nb1 – C1 (bonding)	2.222(3)	2.216(2)
Nb1 – C2 (terminal)	2.264(3)	2.266(2)
C1 – N1 (bonding)	1.139(4)	1.150(3)
C2 – N2 (terminal)	1.140(4)	1.149(3)
\angle Nb1 – C1 – N1	178.6(3)	178.7(2)
\angle Nb1 – C2 – N2	178.3(4)	177.8(2)
[Mn ^{II} (4-Clpy) ₄ (NC) ₂] moiety		
Mn1 – N1 (CN)	2.115(3)	2.107(2)
Mn1 – N3 (Clpy)	2.343(3)	2.315(2)
Mn1 – N4 (Clpy)	2.326(3)	2.332(2)
\angle Mn1 – N1 – C1	170.5(3)	169.1(2)
\angle N3(Clpy) – Mn – N3(Clpy)	180	180
\angle N4(Clpy) – Mn – N4(Clpy)	180	180
\angle N3(Clpy) – Mn – N4(Clpy)	89.32(11), 90.67(11)	89.04(7), 90.96(7)
\angle N(Clpy) – Mn – N(CN)	89.13(11) – 90.87(11)	88.91(8) – 91.09(8)

Table S2. Detailed Structural Parameters (continued)

compound	Mn-Nb-4-Brpy network (+)	Mn-Nb-4-Brpy network (+) ^{S5}	Mn-Nb-4-Brpy network (-)	Mn-Nb-4-Brpy network (-) ^{S5}
Temperature	90 K	293	90	293
Halogen Bonding				
N2...Br1	3.087(3)	3.156(5)	3.078(4)	3.161(9)
∠N2...Br1 – C5	170.78(11)	171.7(2)	170.96(19)	171.8(4)
[Nb ^{IV} (CN) ₈] moiety				
Nb1 – C1 (bonding)	2.220(3)	2.225(4)	2.214(5)	2.229(7)
Nb1 – C2 (terminal)	2.262(3)	2.256(5)	2.270(5)	2.260(7)
C1 – N1 (bonding)	1.153(4)	1.140(6)	1.153(6)	1.141(8)
C2 – N2 (terminal)	1.143(4)	1.141(6)	1.145(6)	1.131(8)
∠Nb1 – C1 – N1	178.5(3)	179.6(5)	178.9(5)	179.9(8)
∠Nb1 – C2 – N2	178.8(3)	179.5(5)	178.6(5)	179.6(8)
[Mn ^{II} (4-Brpy) ₄ (NC) ₂] moiety				
Mn1 – N1 (CN)	2.111(3)	2.125(4)	2.109(4)	2.115(6)
Mn1 – N3 (Brpy)	2.317(4)	2.323(4)	2.321(4)	2.331(6)
Mn1 – N4 (Brpy)	2.356(4)	2.336(6)	2.352(6)	2.324(9)
Mn1 – N5 (Brpy)	2.317(4)	2.352(6)	2.321(7)	2.333(10)
∠Mn1 – N1 – C1	166.4(3)	168.9(4)	166.8(5)	168.9(6)
∠N3(Brpy) – Mn – N3(Brpy)	171.60(14)	172.8(2)	171.7(2)	173.4(3)
∠N3(Brpy) – Mn – N4(Brpy)	94.20(7)	93.63(10)	94.14(12)	93.30(16)
∠N3(Brpy) – Mn – N5(Brpy)	85.80(7)	86.37(10)	85.86(12)	86.70(16)
∠N4(Brpy) – Mn – N5(Brpy)	180	180	180	180
∠N(CN) – Mn – N(CN)	176.32(15)	176.9(2)	176.6(3)	176.8(4)
∠N(Brpy) – Mn – N(CN)	88.16(7)–91.84(7)	88.45(12)–91.55(12)	88.30(13)–91.70(13)	88.40(18)–90.9(20)

Table S3. Results of Continuous Shape Measures (CShM) Analysis of $[\text{Nb}^{\text{IV}}(\text{CN})_8]^{4-}$ (top) and $[\text{Mn}^{\text{II}}(\text{NC})_2(4\text{-halopyridine})_4]$ moieties (bottom).

Nb ^{IV} ion		CShM parameters			Geometry
		BTP-8	SAPR-8	DD-8	
1(+)	RT	1.934	0.183	2.052	SAPR-8
	90 K	2.191	0.118	2.500	SAPR-8
1(-)	RT	1.955	0.170	2.117	SAPR-8
	90 K	2.183	0.115	2.497	SAPR-8
2	RT	2.007	0.155	2.115	SAPR-8
	90 K	2.221	0.120	2.576	SAPR-8

Mn ^{II} ion		CShM parameters		Geometry
		OC-6	TPR-6	
1(+)	RT	0.193	15.409	OC-6
	90 K	0.254	15.252	OC-6
1(-)	RT	0.242	14.843	OC-6
	90 K	0.241	15.252	OC-6
2	RT	0.216	16.681	OC-6
	90 K	0.218	16.643	OC-6

CShM parameters.

BTP-8 = the parameter related to the bicapped trigonal prism geometry (C_{2v} symmetry)

SAPR-8 = the parameter related to the square antiprism (D_{4d} symmetry)

DD-8 = the parameter related to the dodecahedron (D_{2d} symmetry)

OC-6 = the parameter related to the octahedron (O_h symmetry)

TPR-6 = the parameter related to the trigonal prism (D_{3h} symmetry)

CShM parameter is 0 for the ideal geometry and increases when distortion from the ideal polyhedron increase.

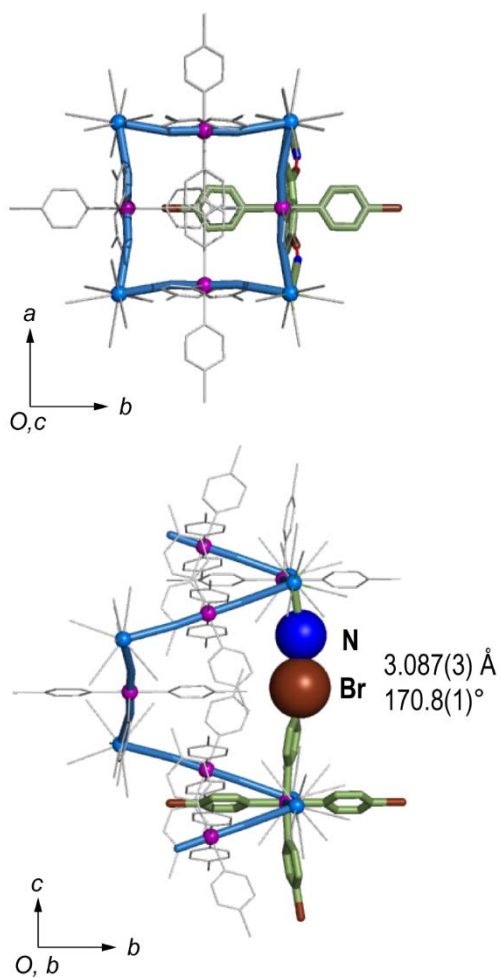


Figure S1. Helix of the Mn-Nb-4-Brpy network at 90 K. Top (upper) and side (bottom) views. The angle indicates $\angle\text{NBrC}$. Purple sphere, blue sphere, blue, and brown represent Mn, Nb, N, and Br, respectively.

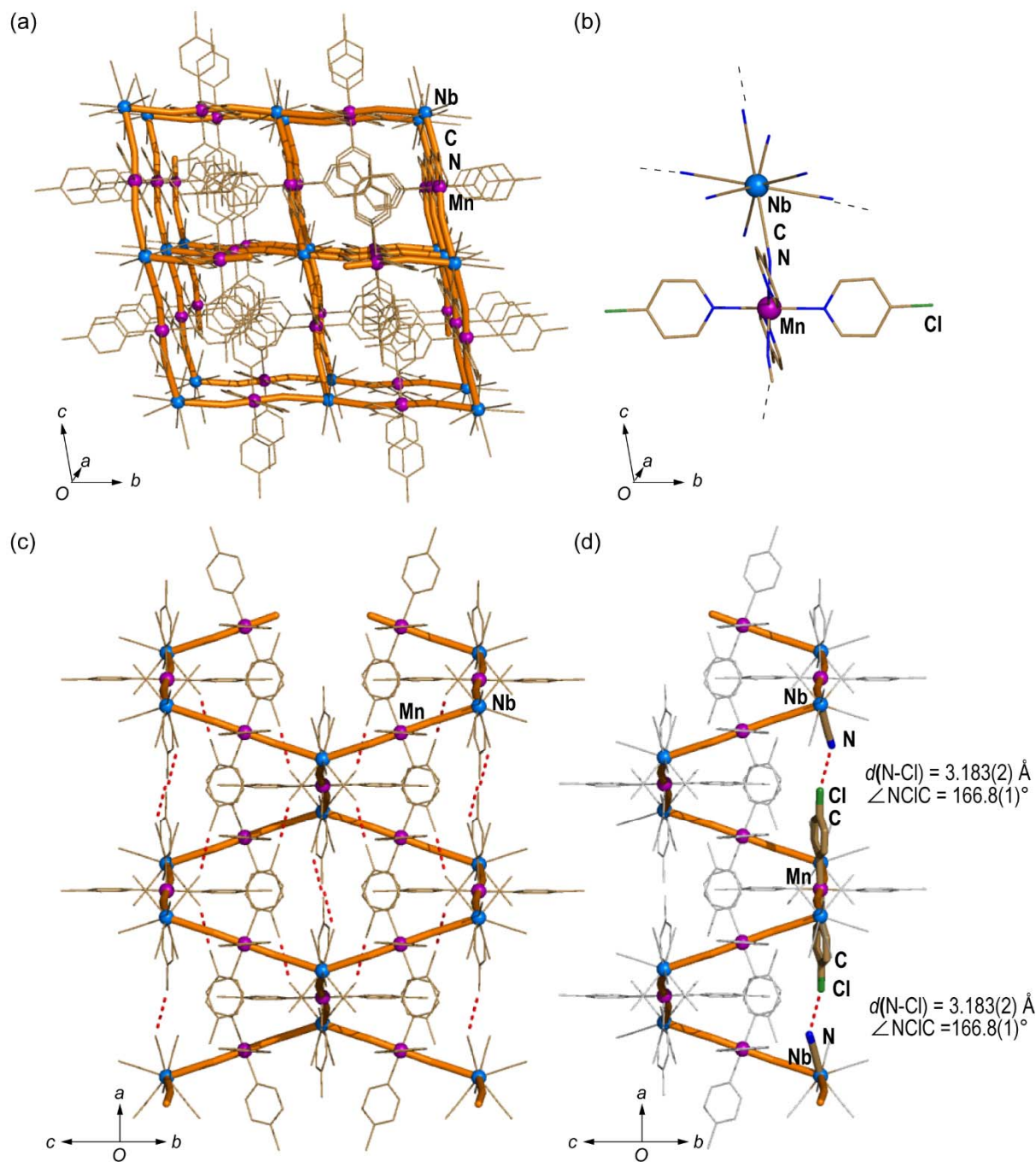


Figure S2. Crystal structure of **2** at 90 K. (a) View along the *a*-axis. (b) Coordination geometry around Mn^{II} and Nb^{IV} . (c) Projection along the *b*-axis. (d) View focusing the halogen bonding. Purple sphere, blue sphere, light brown, blue, and green represent Mn, Nb, C, N, and Cl atoms, respectively. Orange helices show the left-handed and the right-handed ones. Red dashed lines stand for the halogen bonds between chlorine and nitrogen atoms.

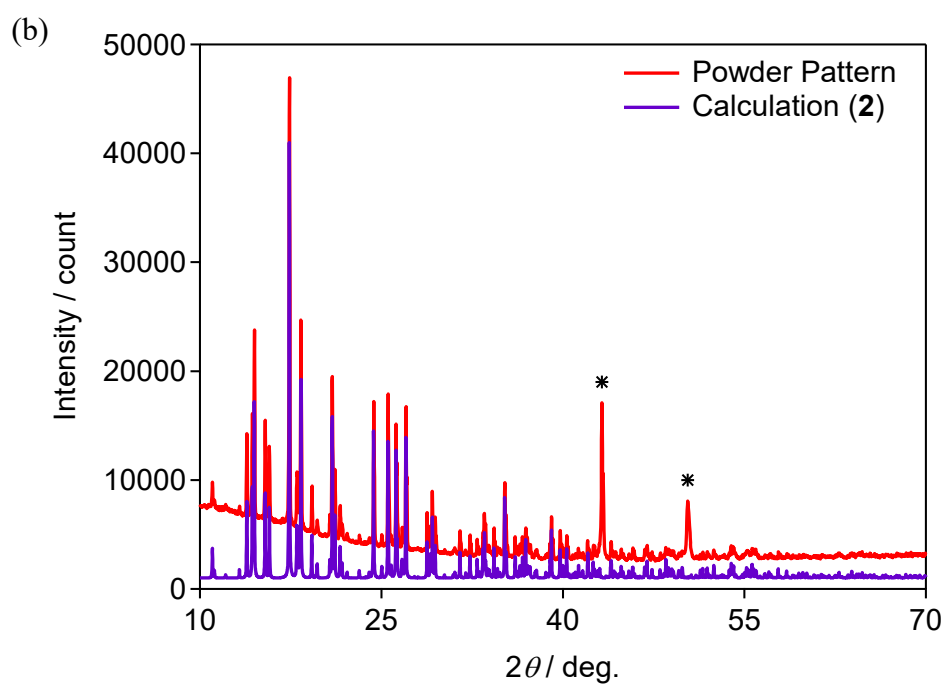
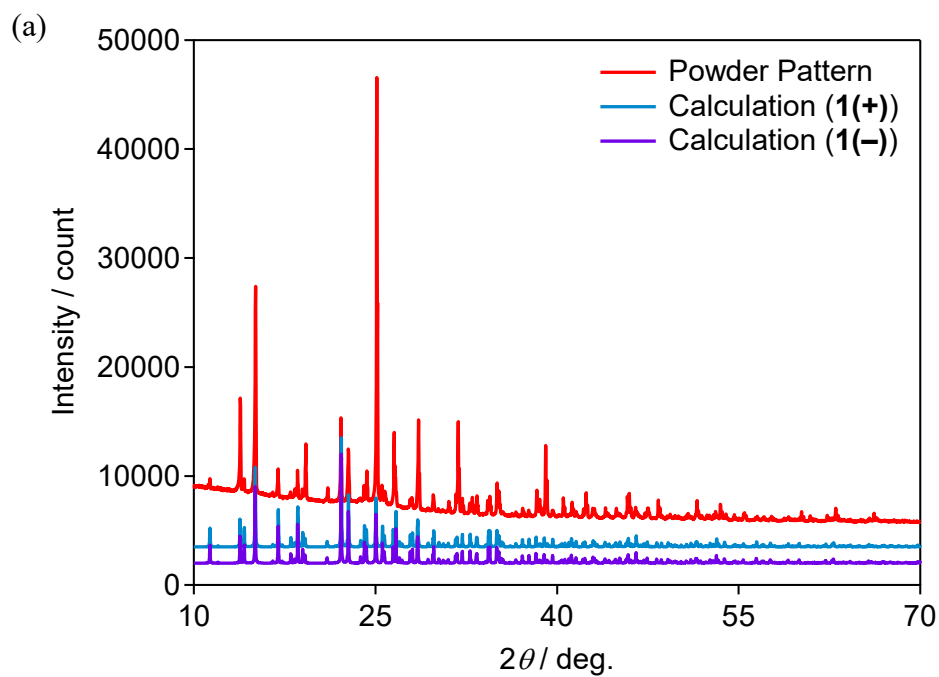


Figure S3. Powder X-ray diffraction patterns of **1** (a) and **2** (b) with calculated patterns based on single crystal structural analyses. The pattern of **2** was obtained under nitrogen atmosphere and contains peaks of a Cu sample plate (asterisk).

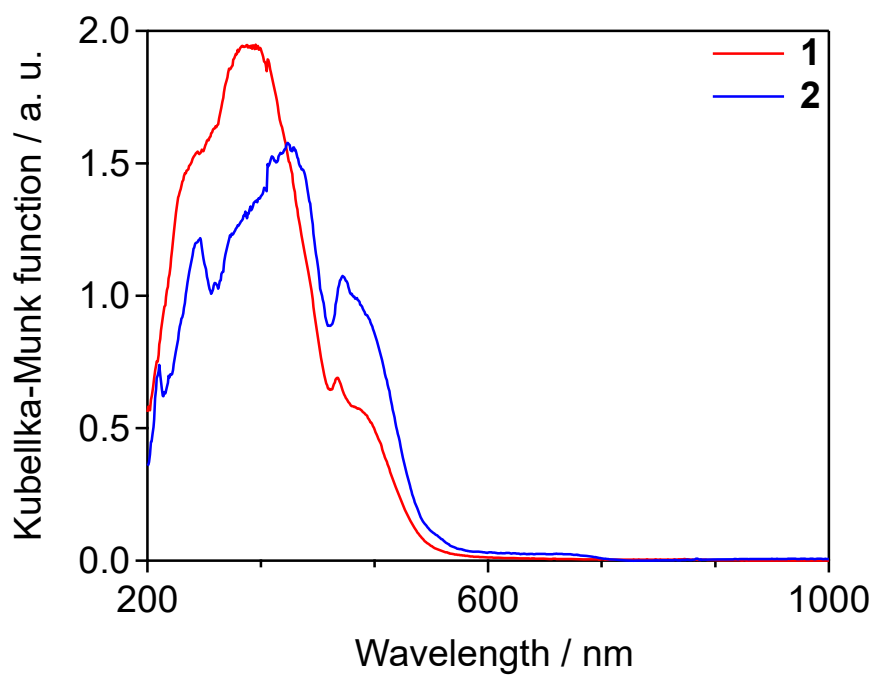


Figure S4. UV-Vis diffuse reflectance spectra of **1** and **2**

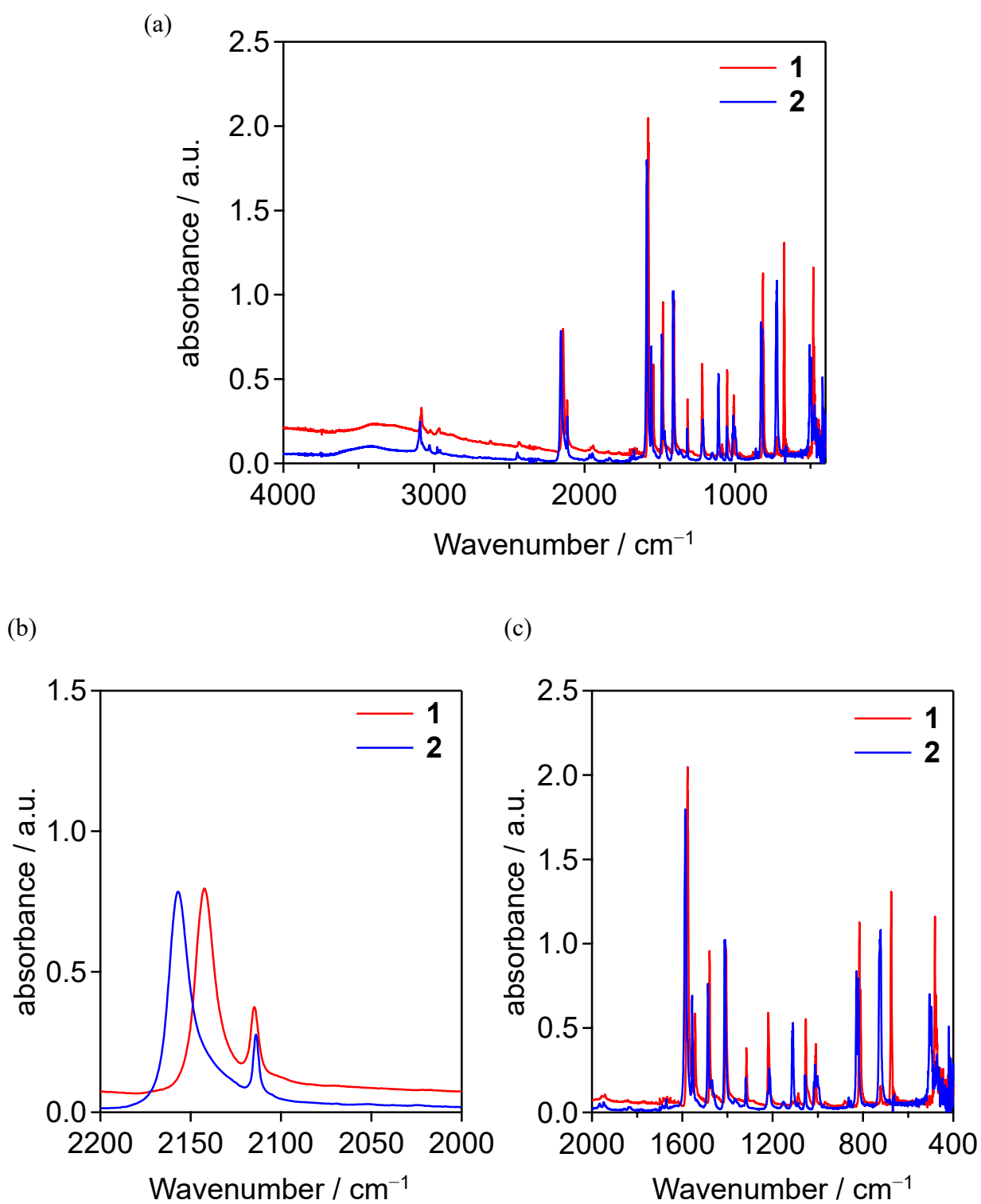
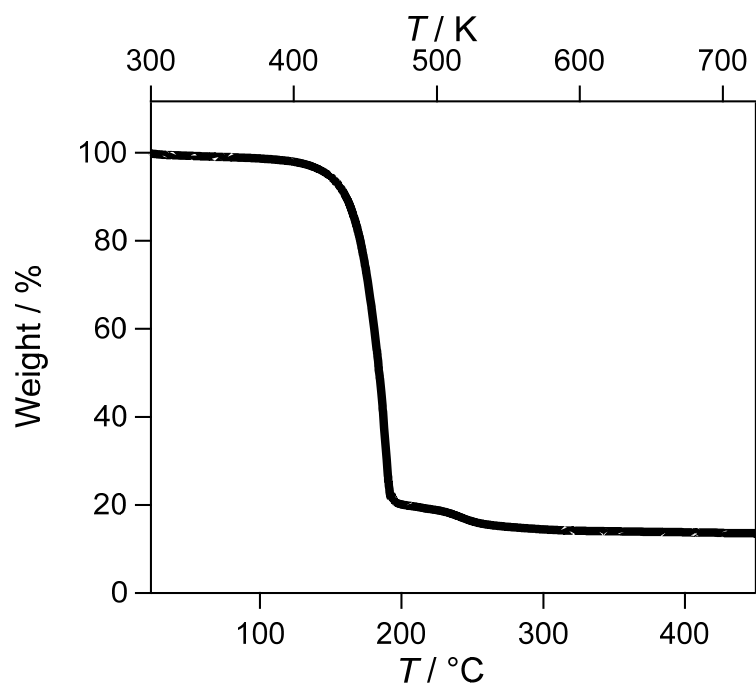


Figure S5. IR spectra of **1** and **2**. (a) Total view, (b) CN stretching region and (c) fingerprint region.

(a)



(b)

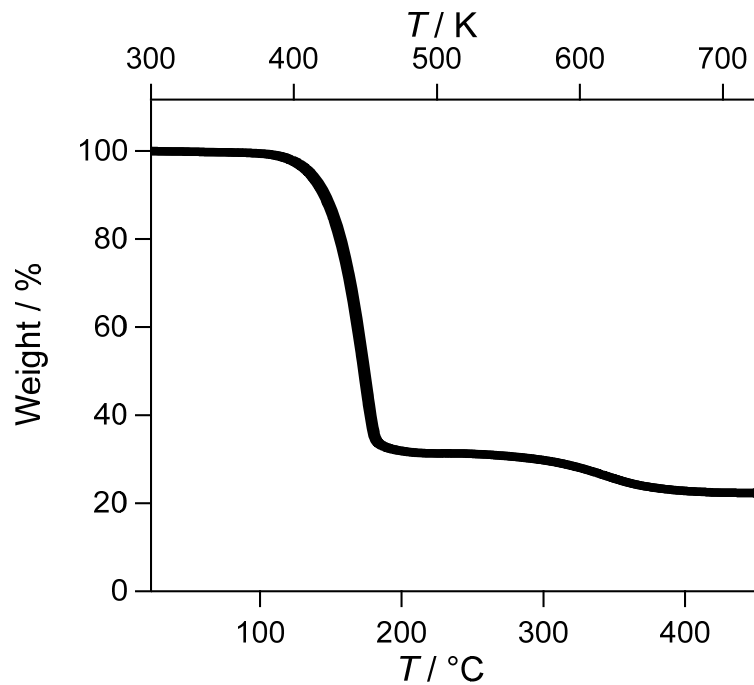


Figure S6. Results of thermogravimetric measurements for **1** (a) and **2** (b) in the 27–450 °C range under a scan rate of 2 °C per minute.

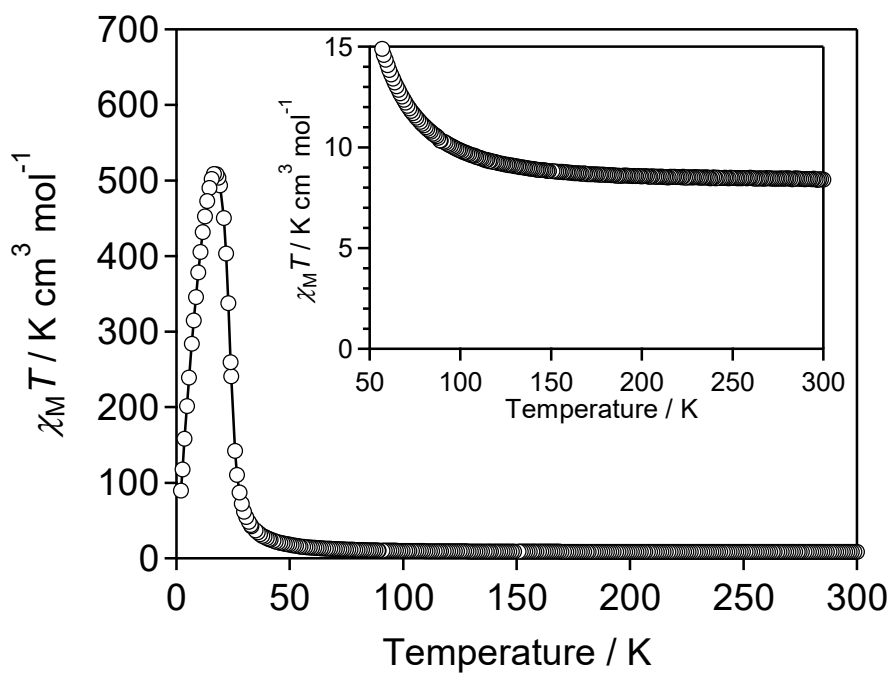


Figure S7. Temperature dependence of $\chi_M T$ of **1** in the applied dc magnetic field of 1000 Oe. Inset shows an enlarged view of the $\chi_M T$ plot.

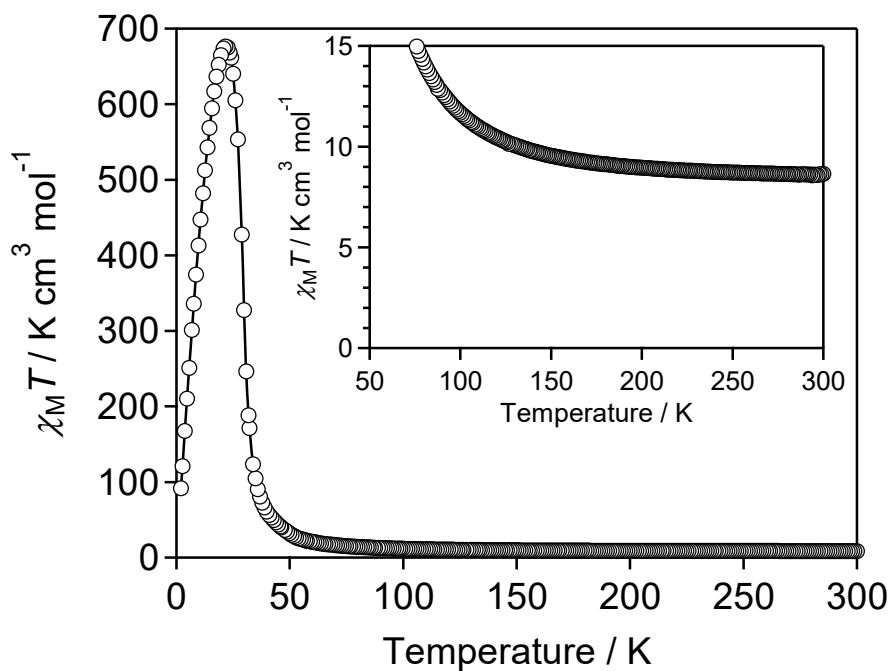


Figure S8. Temperature dependence of $\chi_M T$ of **2** in the applied dc magnetic field of 1000 Oe. Inset shows an enlarged view of the $\chi_M T$ plot.

Tensor elements of the SH susceptibility for 1 and Mn-Nb-4-Brpy network.

In the space group of $I4_1$ (crystallographic point group: 4) for **1**, the nonzero elements in crystallographic term, (χ_{ijk}) : χ_{zxx} , χ_{zyy} , χ_{zzz} , χ_{xyz} , and χ_{xxz} appear. Based on the relationship, $P_i = \chi_{ijk}E_jE_k$, the SH susceptibility in this system is expressed by the following equation.

$$\begin{pmatrix} P_x \\ P_y \\ P_z \end{pmatrix} = \begin{pmatrix} 0 & 0 & 0 & \chi_{xyz} & \chi_{xxz} & 0 \\ 0 & 0 & 0 & \chi_{yyz} & \chi_{yxx} & 0 \\ \chi_{zxx} & \chi_{zyy} & \chi_{zzz} & 0 & 0 & 0 \end{pmatrix} \begin{pmatrix} E_x^2 \\ E_y^2 \\ E_z^2 \\ 2E_yE_z \\ 2E_zE_x \\ 2E_xE_y \end{pmatrix}$$

, where $\chi_{zxx} = \chi_{zyy}$, $\chi_{xxz} = \chi_{yyz}$, and $\chi_{yxx} = -\chi_{yzz}$.

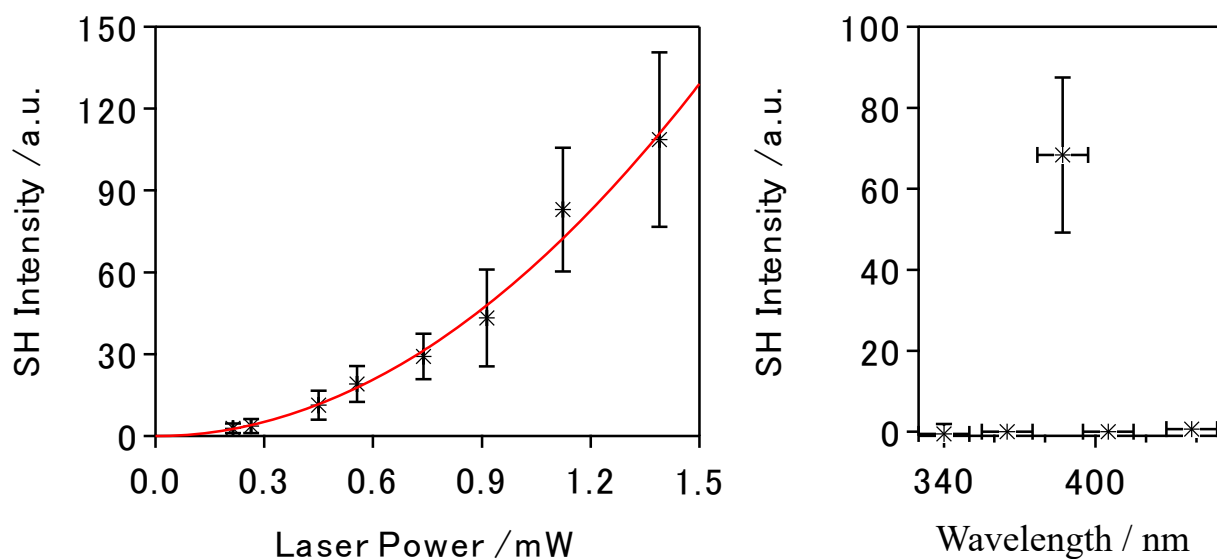
In the system of $I4_122$ (crystallographic point group: 422) for the Mn-Nb-4-Brpy network, the SH susceptibility is expressed by the following equation.

$$\begin{pmatrix} P_x \\ P_y \\ P_z \end{pmatrix} = \begin{pmatrix} 0 & 0 & 0 & \chi_{xyz} & 0 & 0 \\ 0 & 0 & 0 & 0 & \chi_{yxx} & 0 \\ 0 & 0 & 0 & 0 & 0 & 0 \end{pmatrix} \begin{pmatrix} E_x^2 \\ E_y^2 \\ E_z^2 \\ 2E_yE_z \\ 2E_zE_x \\ 2E_xE_y \end{pmatrix}$$

, where $\chi_{yxx} = -\chi_{yzz}$.

Thus, the SH light of **3** is derived only from the contributions of χ_{xyz} and χ_{yxx} .

(a)



(b)

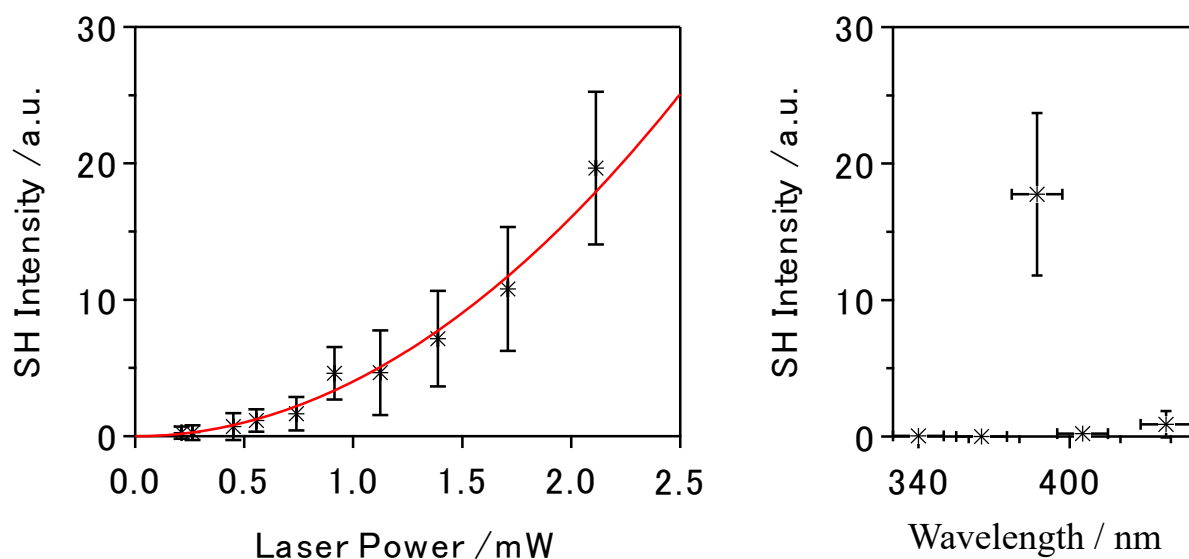


Figure S9. The SH light intensity vs fundamental light intensity plots of **1** (a) and the Mn-Nb-4-Brpy network (b). Left plots show the dependence of the incident laser power and the red solid line represents a quadratic function of the fundamental light intensity. Right plots show the dependence of measured wavelength and horizontal error bars mean half width of the bandpass filters. Wavelength of the incident light is 775 nm.

REFERENCES TO SUPPORTING INFORMATION

- [S1] (a) A. Altomare, G. Cascarano, C. Giacovazzo, A. Guagliardi, *J. Appl. Cryst.*, **1993**, *26*, 343–350. (b) M. C. Burla, R. Caliandro, B. Carrozzini, G. Cascarano, C. Cuocci, C. Giacovazzo, M. Mallamo, A. Mazzone, G. Polidori, *J. Appl. Cryst.*, **2015**, *48*, 306–309.
- [S2] G. M. Sheldrick, *Acta Cryst.*, **2008**, *A64*, 112–122.
- [S3] L. J. Farrugia, *J. Appl. Cryst.*, **2012**, *45*, 849–854.
- [S4] (a) D. Casanova, J. Cirera, M. Llunell, P. Alemany, D. Avnir, S. Alvarez, *J. Am. Chem. Soc.*, **2004**, *126*, 1755–1763. (b) M. Llunell, D. Casanova, J. Cirera, J. Bofill, P. Alemany, S. Alvarez, M. Pinsky, D. Avnir, *SHAPE v. 2.1. Program for the Calculation of Continuous Shape Measures of Polygonal and Polyhedral Molecular Fragments*; University of Barcelona: Barcelona, Spain, **2013**.
- [S5] T. Ohno, S. Chorazy, K. Imoto, S. Ohkoshi, *Cryst. Growth Des.*, **2016**, *16*, 4119–4128.